

# Heavy Quarks at the Tevatron: Top & Bottom

Manfred Paulini (Representing the CDF and DØ Collaboration) <sup>§</sup>

Lawrence Berkeley National Laboratory, Berkeley, CA 94720, USA

## Abstract

We review the status of heavy quark physics at the Fermilab Tevatron collider by summarizing recent top quark and  $B$  physics results from CDF and DØ. In particular, we discuss the measurement of the top quark mass and top production cross section as well as  $B$  meson lifetimes and time dependent  $B^0\bar{B}^0$  mixing results.

## 1 Introduction

In this report, we review recent results on heavy quark physics (top & bottom) from the Tevatron  $p\bar{p}$  collider at Fermilab operating at a centre-of-mass energy of  $\sqrt{s} = 1.8$  TeV. During the Tevatron Run I, which ended in 1996, the CDF experiment [1] and the DØ detector [2] recorded each an integrated luminosity of about  $100 \text{ pb}^{-1}$ .

In Section 2, we summarize the status of top quark physics at CDF and DØ discussing measurements of the top production cross section and the top quark mass. Section 3 is devoted to recent  $B$  physics results from the Tevatron collider, where we concentrate on  $B$  hadron lifetimes and time dependent  $B^0\bar{B}^0$  mixing results. We conclude with Section 4.

## 2 Top Quark Physics at the Tevatron

At the Tevatron the dominant top quark production mechanism is  $t\bar{t}$  pair production through  $q\bar{q}$  annihilation. Gluon-gluon fusion contributes to the  $t\bar{t}$  cross section to about 10% at  $\sqrt{s} = 1.8$  TeV. During the Tevatron Run I over  $5 \cdot 10^{12}$   $p\bar{p}$  collisions took place within the CDF and DØ detectors but only about 500  $t\bar{t}$  pairs have been produced per experiment implying  $\sigma_{t\bar{t}}$  to be about ten orders of magnitudes lower than the total inelastic cross section. This means the challenge in studying top quarks is to separate them from backgrounds in hadronic collisions.

Within the Standard Model, each of the pair produced top quarks decays almost exclusively into a  $W$  boson and a  $b$  quark. The  $W$  boson decays into either a lepton-neutrino or quark-antiquark pair. The top decay signature depends primarily on the decay of the  $W$  boson. Events are classified by the number of  $W$ 's that decay leptonically.

If both  $W$  bosons decay leptonically into  $W \rightarrow \ell\nu$ , where lepton  $\ell$  refers to  $e$  or  $\mu$ , we call it the ‘dilepton channel’. The final state consists of  $\ell^-\bar{\nu}\ell^+\nu b\bar{b}$  as can be seen in Figure 1a). Due to both  $W$ 's decaying semileptonically, this top decay mode has a small branching fraction of about 5%. If one of the  $W$  bosons decays leptonically into  $W \rightarrow \ell\nu$  and the other into  $W \rightarrow q\bar{q}'$ , we call it the ‘lepton plus jets channel’, where the final state consists of  $\ell\nu q\bar{q}' b\bar{b}$  as shown in Figure 1b). This decay mode happens with a branching ratio of about 30%. If both  $W$  bosons decay into quark pairs as  $W \rightarrow q\bar{q}'$ , we call it the ‘all hadronic channel’. The final state consists of  $q\bar{q}' q\bar{q}' b\bar{b}$  as can be seen in Fig. 1c). This top decay mode occurs at a large rate of about 44%. The remaining top decays involve a  $\tau$  lepton plus another lepton (6%) or a  $\tau$  lepton plus jets (15%).

<sup>§</sup>To appear in the Proceedings of IVth International Workshop on Progress in Heavy Quark Physics, Rostock, Germany, 20-22 September 1997.

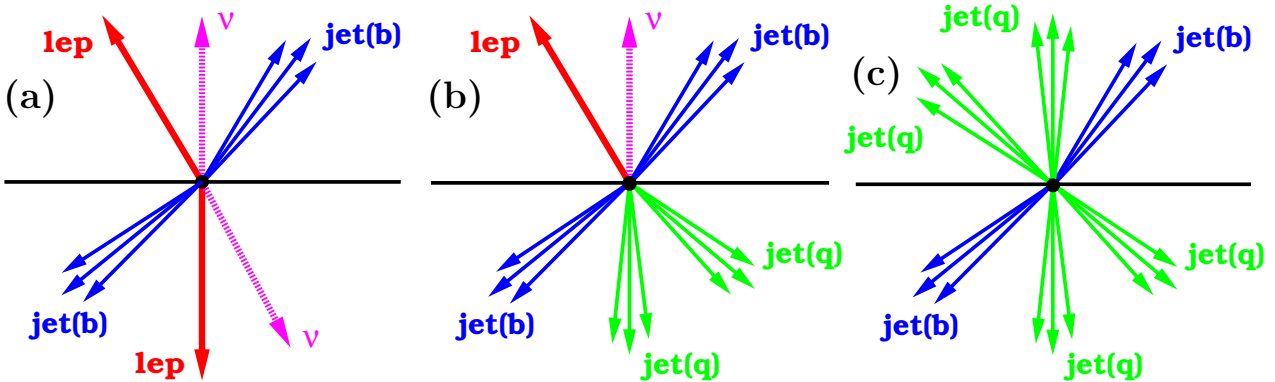


Figure 1: Top decay signature of (a) the dilepton channel, (b) the lepton plus jets channel, and (c) the all hadronic channel.

Dilepton	DØ	CDF	Lepton plus jets	DØ	CDF
<u><math>e\mu</math>:</u>	3	7	Event shape:	19	22
Background	$0.2 \pm 0.2$	$0.8 \pm 0.2$	Background	$8.7 \pm 1.7$	$7.2 \pm 2.1$
Expected yield	$2.2 \pm 0.5$	$2.6 \pm 0.2$	Expected yield	$14.1 \pm 3.1$	$(67 \text{ pb}^{-1})$
<u><math>ee</math> or <math>\mu\mu</math>:</u>	2	2	Lepton tag:	11	40
Background	$1.2 \pm 0.3$	$1.6 \pm 0.4$	Background	$2.4 \pm 0.5$	$24.3 \pm 3.5$
Expected yield	$1.9 \pm 0.3$	$1.8 \pm 0.2$	Expected yield	$5.8 \pm 1.0$	$9.6 \pm 1.7$
<u><math>e\nu</math> (DØ), <math>\ell\tau</math> (CDF):</u>	4	4	SVX tag:	-	34
Background	$1.2 \pm 0.4$	$2.0 \pm 0.4$	Background	-	$8.0 \pm 1.4$
Expected yield	$1.7 \pm 0.5$	$0.7 \pm 0.1$	Expected yield	-	$19.8 \pm 4.0$

Table 1: Event summary for the dilepton channel (left) and the lepton plus jets channel (right). The expected yield from  $t\bar{t}$  production is based on determinations of the top cross section [3] for a top quark mass of  $170 \text{ GeV}/c^2$  (DØ) and  $175 \text{ GeV}/c^2$  (CDF), respectively.

## 2.1 The Counting Experiments

### 2.1.1 The Top Dilepton Channel

The signature of the dilepton channel (see Fig. 1a) is two isolated high  $p_t$  leptons and missing energy ( $\cancel{E}_t$ ) from the two neutrinos that escape the detector unobserved. In addition, there are two jets originating from  $b$  quarks in the event. After demanding two leptons and  $\cancel{E}_t$ , the event selection also relies on kinematic requirements. The dominant backgrounds are from Drell-Yan production,  $Z \rightarrow \tau\tau$ , fake leptons, and  $WW$  diboson production. The dilepton channel has a good signal to background ratio, but low statistics. The dilepton event summary for CDF and DØ is shown in Table 1 (left) and further described in Ref. [4, 5]. Both experiments find a few events on small backgrounds. Table 1 also contains the DØ  $e\nu$  channel [6] and the CDF  $e$  or  $\mu$  plus  $\tau$  mode [7].

### 2.1.2 The Top Lepton plus Jets Channel

The signature of the lepton plus jets channel (see Fig. 1b) is one isolated high  $p_t$  lepton, missing energy ( $\cancel{E}_t$ ) from the neutrino and four jets where two of them are from  $b$  quarks. The dominant background is from  $W$  plus jet production, where the jets tend to be softer than jets in  $t\bar{t}$  events. In addition,  $t\bar{t}$  events always contain  $b$  quarks. Both experiments follow different strategies to reduce the background in this channel.

CDF tags the  $b$  jets in the event through a ‘soft lepton tag’ (SLT) and a ‘SVX tag’. The first technique identifies  $b$  jets by searching for typically low momentum leptons from  $b \rightarrow \ell X$  or  $b \rightarrow c \rightarrow \ell X$  decays. Electrons and muons are found by matching tracks from the central drift chamber with electromagnetic energy clusters in the calorimeter or track segments in the muon chambers. The efficiency for SLT tagging a  $t\bar{t}$  event is  $(18 \pm 2)\%$  with a typical mistag rate per jet of about 2%. Details of the SLT algorithm can be found in Ref. [8]. The second, more powerful  $b$  tagging technique (SVX tag) exploits the finite lifetime of  $b$  hadrons by searching for a secondary decay vertex displaced from the primary event vertex with CDF’s silicon vertex detector. The efficiency for SVX tagging a  $t\bar{t}$  event is  $(39 \pm 3)\%$ , while the mistag rate is only  $\approx 0.5\%$ . More information on the SVX tag can be found in Ref. [8, 9].

DØ uses kinematic and topological cuts as well as  $b$  tagging via soft muon tagging to reduce the background in the lepton plus jets channel. The first approach exploits the fact that jets from  $t\bar{t}$  decays tend to be more energetic and more central than from typical QCD background events. In addition,  $t\bar{t}$  events are more spherical while QCD jet production results in more planar event shapes. Top enriched data samples can therefore be selected with a set of topological and kinematic cuts like missing energy or aplanarity. The second DØ approach uses  $b$  tagging via muon tags through  $b \rightarrow \mu X$  and  $b \rightarrow c \rightarrow \mu X$  decays. For more details on both techniques see Ref. [10, 11]. The lepton plus jets event summary for the CDF and DØ experiment is shown in Table 1 (right).

### 2.1.3 The Top All Hadronic Channel

The signature of the all hadronic channel (Fig. 1c) is nominally six jets where two of them are from  $b$  quarks, no leptons, and low  $\cancel{E}_t$ . In order to overcome the huge background from QCD multijet production,  $b$  tagging as well as kinematic requirements are used. If the backgrounds can be controlled, the all hadronic channel would be well suited to determine the top mass because all objects of the top decay are measured in the detector.

After kinematic cuts are applied in the CDF all hadronic analysis [12], at least five jets are required, where the leading jets have to pass an aplanarity cut. In addition, at least one jet has to be SVX tagged. CDF observes 187 events on a predicted background of  $151 \pm 10$  events. In the search for  $t\bar{t}$  events in the all hadronic mode, DØ requires six jets, where a soft muon tag has to be present in at least one of the jets. DØ combines several kinematic variables and uses a neural net approach to separate signal from background obtaining 44 events with an expected background of  $25.3 \pm 7.3$  events.

## 2.2 The Top Production Cross Section

The measurement of the top production cross section is given by  $\sigma_{t\bar{t}} = (N_{\text{obs}} - N_{\text{bkg}})/A \mathcal{L}$ . The number of predicted background events  $N_{\text{bkg}}$  is subtracted from the number of observed top candidates  $N_{\text{obs}}$  and divided by the acceptance  $A$  of the sample selection and the integrated luminosity  $\mathcal{L}$  of the used data set. The measurement of  $\sigma_{t\bar{t}}$  has been determined in several decay channels. The results of the different  $\sigma_{t\bar{t}}$  measurements from CDF [13] are  $8.2^{+4.4}_{-3.4}$  pb,  $6.7^{+2.0}_{-1.7}$  pb, and  $10.1^{+4.5}_{-3.6}$  pb for the dilepton, lepton plus jets, and all hadronic mode, respectively. CDF measures a combined top production cross section of  $\sigma_{t\bar{t}} = 7.6^{+1.8}_{-1.5}$  pb. The results from the DØ analysis [6] are  $6.3 \pm 3.3$  pb from the dilepton and  $e\nu$  channel,  $4.1 \pm 2.0$  pb from lepton plus jets, and  $8.2 \pm 3.5$  pb from lepton plus jets

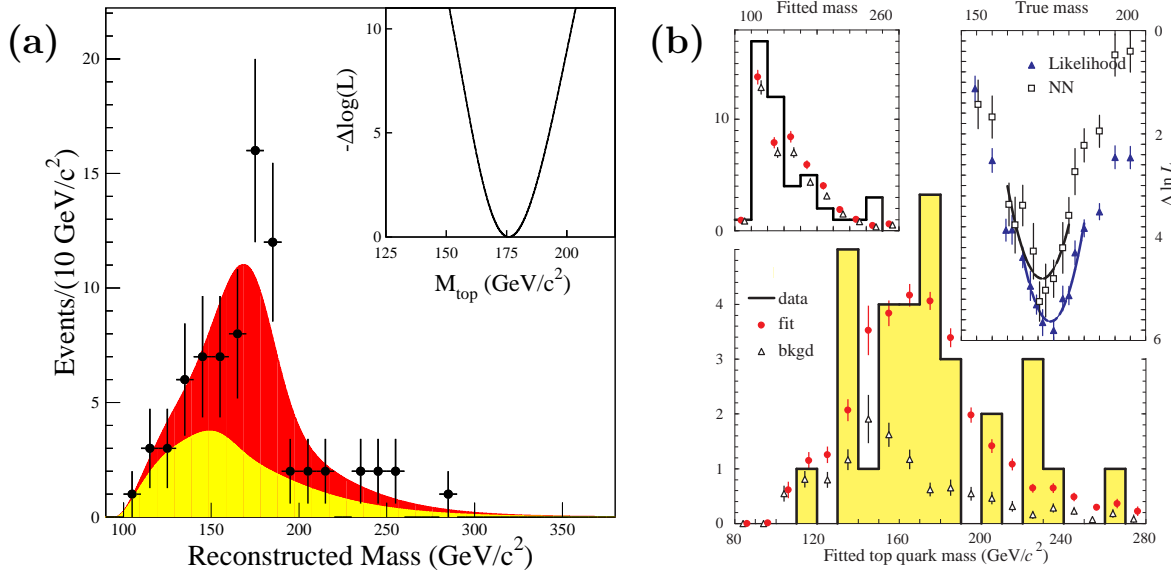


Figure 2: Reconstructed mass distribution of (a) the CDF and (b) the DØ top quark mass measurements in the lepton plus jets decay channel. See text for more information.

with a  $\mu$  tag. DØ quotes a combined top cross section of  $\sigma_{t\bar{t}} = (5.5 \pm 1.8)$  pb. Theoretical predictions [3, 14] range between 4.7–5.5 pb for a top quark mass of 175 GeV/c<sup>2</sup>.

### 2.3 The Top Quark Mass Measurement

The top quark mass  $m_{\text{top}}$  is a fundamental parameter of the Standard Model. A precise determination of  $m_{\text{top}}$  is one of the most important measurement of CDF and DØ in Run I. Because of the large background in the all hadronic mode and the low number of top events in the dilepton channel, the most powerful dataset for measuring the top quark mass is the lepton plus jets sample. The preferred method to determine  $m_{\text{top}}$  is a constrained fit to the lepton plus 4-jet events arising from the process  $t\bar{t} \rightarrow WbW\bar{b} \rightarrow \ell\nu b\bar{q}\bar{q}'\bar{b}$ . The exact correspondence between the observed lepton, jets, and  $\not{E}_t$  and the  $t\bar{t}$  decay products is not known. There are 12 combinations to assign the observed objects to the partons from the  $t\bar{t}$  decay. These are reduced to six (two) combinations if one (two)  $b$  jets are tagged. Usually the mass fitter decides on a preferred assignment based on a  $\chi^2$  variable.

At CDF the lepton plus 4-jet sample with at least one SVX tag provided the original top mass measurement [9]. Optimization studies indicated a reduced error on  $m_{\text{top}}$ , if the tagged events are partitioned into non-overlapping tagging classes and a set of untagged events is added. The following four data samples are used: events with a single SVX tag (15 events), events with two SVX tags (5 events), events with a SLT tag but no SVX tag (14 events), and events with no tag but all four leading jets have  $E_t > 15$  GeV (42 events). The reconstructed mass distribution of the sum of the four subsamples is plotted in Fig. 2a). The data points are compared with the result of the combined fit (dark shading) and the fitted background component (light shading). The inset shows the shape of the log-likelihood as a function of  $m_{\text{top}}$ . A value of  $m_{\text{top}} = (175.9 \pm 4.8 \pm 4.9)$  GeV/c<sup>2</sup> has been extracted, where the main systematic error is from the jet energy scale. Further details on the CDF top quark mass measurement can be found in Ref. [15].

The DØ top mass measurement [11] is based on 77 lepton plus jets events, where five events are  $\mu$  tagged and about 65% are background. Further separation of signal and background

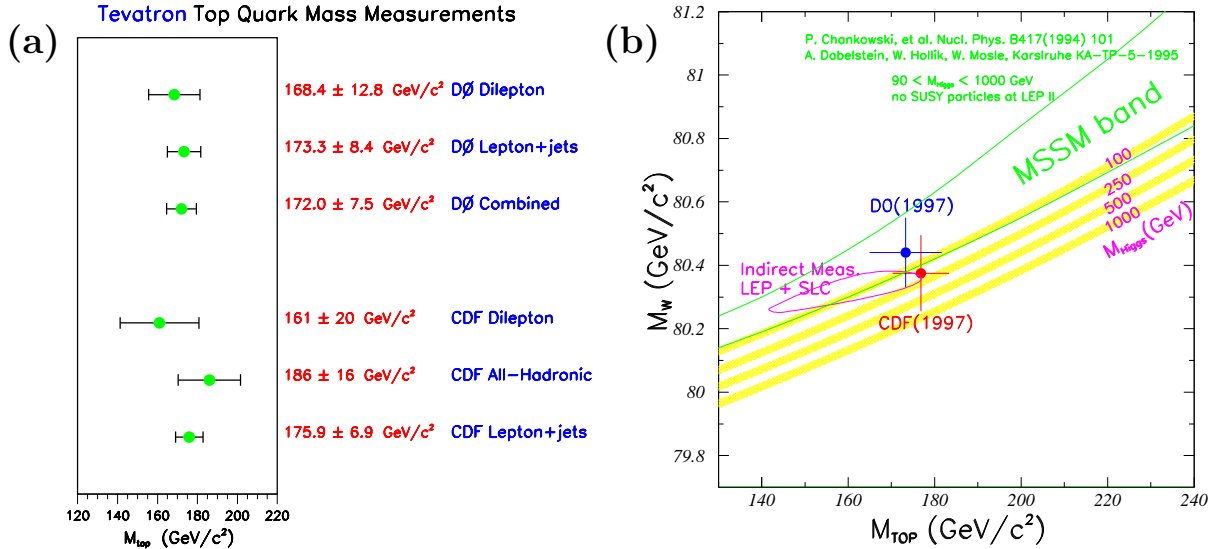


Figure 3: (a) Summary of the CDF and DØ top quark mass measurements in different decay channels. (b) Relation between the top quark mass and the  $W$  boson mass.

is based on four kinematic variables, which are chosen to have small correlations with  $m_{\text{top}}$ . DØ also engages in a neural net approach, which is sensitive to these kinematic variables as well as their correlations. The reconstructed top mass distribution of the final lepton plus jets sample is shown in Fig. 2b). The shaded histogram are the data, while the solid circles represent the predicted mixture of top and background, and the triangles are the predicted background only. DØ extracts  $m_{\text{top}} = (173.3 \pm 5.6 \pm 6.2) \text{ GeV}/c^2$ , where the main systematic error also comes from the jet energy scale.

A summary of the top quark mass measurement by CDF and DØ is shown in Figure 3a). Both experiments also measured  $m_{\text{top}}$  in the dilepton channel, while CDF has a top mass determination from the all hadronic channel [12] in addition.

Since the top quark mass is large, it controls the strength of quark loop corrections to electroweak parameters like the  $W$  boson mass  $m_W$ . If  $m_{\text{top}}$  and  $m_W$  are precisely measured, the Standard Model Higgs boson mass can be constraint as shown in Fig. 3b). The Tevatron results as well as the indirect measurements at the  $Z$  pole seem to indicate a small Higgs boson mass, but the uncertainties are still large and more data is needed.

### 3 Bottom Quark Physics at the Tevatron

The principal interest in studying  $B$  hadrons in the context of the Standard Model arises from the fact that  $B$  hadron decays provide valuable information on the weak mixing matrix, the Cabibbo-Kobayashi-Maskawa (CKM) matrix [16]. Traditionally,  $B$  physics has been the domain of  $e^+e^-$  machines, but already the UA 1 collaboration has shown that  $B$  physics is feasible at a hadron collider [17]. In this report, we concentrate on recent results on  $B$  hadron lifetimes and time dependent  $B^0\bar{B}^0$  oscillations where there exist only results from the CDF experiment.

The main production mechanism of  $b$  quarks at the Tevatron is through gluon-gluon fusion. Compared to top quark production, the  $b$  quark production cross section is quite large with  $\sigma_b \sim 50 \mu\text{b}$  within the central detector region of rapidity less than one. This huge cross section resulted in about  $5 \cdot 10^9 b\bar{b}$  pairs being produced in Run I. But the

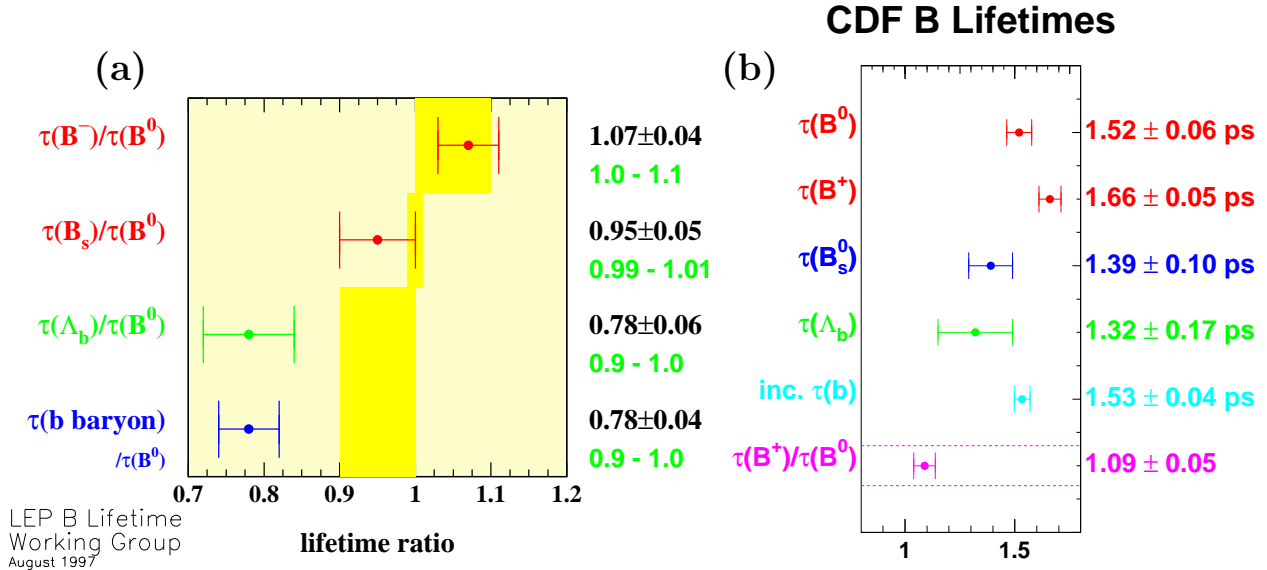


Figure 4: Summary of (a)  $B$  lifetime ratios and (b) CDF  $B$  hadron lifetime measurements.

total inelastic cross section is still about three orders of magnitude larger. This puts certain requirements on the trigger system in finding  $B$  decay products. Because of the rapidly falling  $b$  production cross section, one likes to go as low as possible in the  $p_t$  trigger thresholds to increase the amount of recorded  $B$  triggers with the DAQ bandwidth being the limiting factor. All  $B$  physics triggers at CDF are based on leptons. Dilepton triggers with principal  $p_t$  thresholds of about 2 GeV/c per lepton as well as single lepton triggers with  $p_t$  thresholds around 7.5 GeV/c both exist. An additional basis of CDF's  $B$  physics program are the good tracking and vertexing capabilities of the CTC and SVX.

### 3.1 $B$ Hadron Lifetime Measurements

The lifetime differences between bottom flavoured hadrons can probe the  $B$  decay mechanisms which are beyond the simple quark spectator model. In the case of charm mesons, such differences have been observed to be quite large ( $\tau(D^+)/\tau(D^0) \sim 2.5$ ) [18]. Among bottom hadrons, the lifetime differences are expected to be smaller due to the heavier bottom quark mass [19, 20]. Some phenomenological models [19] predict a lifetime difference between the  $B^+$  and  $B^0$  meson of about 5% and between the  $B^0$  and  $B_s^0$  meson of about 1%. A compilation of different  $B$  hadron lifetime ratios as determined by the LEP  $B$  Lifetime Working Group are shown in Fig. 4a). The range of theoretical predictions are indicated as shaded bands in this Figure.

CDF has measured the lifetimes of all  $B$  hadrons by fully or partially reconstructing  $B^0$ ,  $B^+$ , and  $B_s^0$  mesons as well as  $\Lambda_b$  baryons. A compilation of the precise CDF  $B$  hadron lifetime measurements can be found in Fig. 4b). In the following, we will describe the  $B_s^0$  lifetime measurement using  $D_s^- \ell^+$  correlations, which has recently been updated.

#### 3.1.1 $B_s^0$ Meson Lifetime Measurement

The lifetime of the  $B_s^0$  meson is measured at CDF using the semileptonic decay  $B_s^0 \rightarrow D_s^- \ell^+ \nu X$ , where the  $D_s^-$  is reconstructed through its decay modes into  $\phi \pi^-$ ,  $K^{*0} K^-$ ,  $K_S^0 K^-$ , and  $\phi \mu^- \nu$ . For the first 3 decay modes the analysis starts with a single lepton

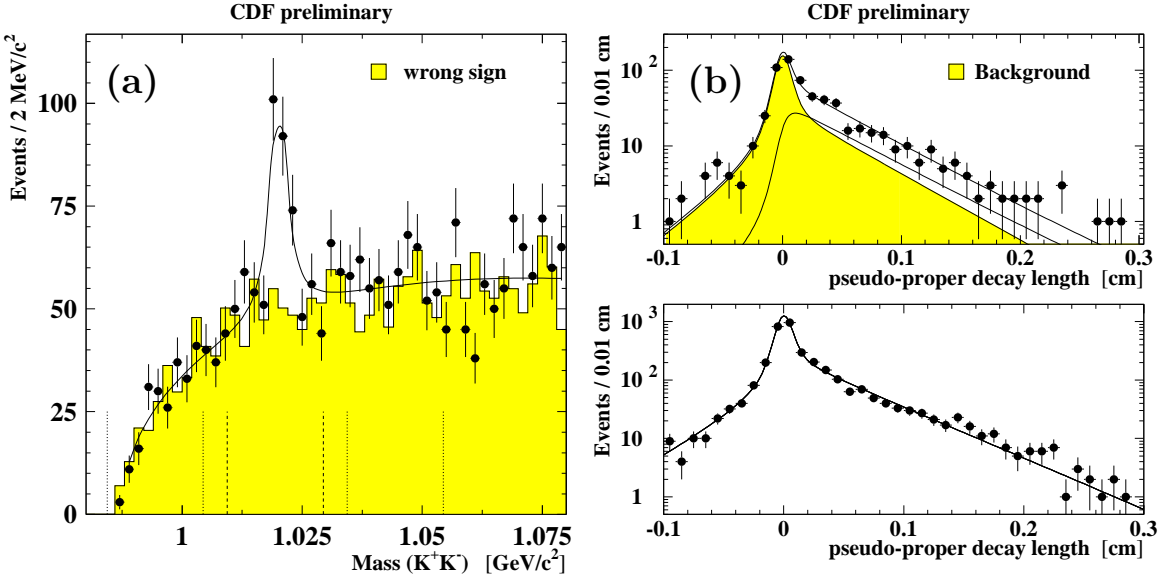


Figure 5: (a) Invariant  $K^+K^-$  mass distribution of  $B_S^0 \rightarrow D_S^- \mu^+ \nu X$  decays with  $D_S^- \rightarrow \phi \mu^- \nu$ ,  $\phi \rightarrow K^+K^-$ . (b) Decay length distributions for signal (top) and background (bottom) in the  $D_S^- \rightarrow \phi \mu^- \nu$  sample.

trigger data set, while the semileptonic  $D_S^-$  decay mode is based on a dimuon data sample obtained with a trigger requirement of  $m(\mu\mu) < 2.8$  GeV/c $^2$ .  $D_S^-$  candidates are searched in a cone around the lepton and then intersected with the lepton to find the  $B_S^0$  decay vertex. Since the  $B_S^0$  meson is not fully reconstructed, its  $c\tau$  cannot be directly determined. A correction has to be applied to scale from the  $D_S^- \ell^+$  momentum to  $p_t(B_S^0)$ . This  $\beta\gamma$  correction is obtained from a Monte Carlo simulation.

About 600  $B_S^0$  candidates have been reconstructed in the four  $D_S^-$  decay channels, where the  $D_S^- \rightarrow \phi\pi^-$  mode contributes the largest statistics with  $220 \pm 21$  events. As an example, the  $K^+K^-$  invariant mass distribution from the  $D_S^- \rightarrow \phi\mu^- \nu$  decay mode with  $\phi \rightarrow K^+K^-$  is shown in Fig. 5a) displaying  $205 \pm 38$  signal events. Figure 5b) shows the decay length distribution of the  $\phi\mu^- \nu$  mode, where the background underneath the  $\phi$  signal was obtained from the  $\phi$  sidebands as displayed at the bottom of Fig. 5b). From all four  $D_S^-$  decay modes a  $B_S^0$  lifetime  $\tau(B_S^0) = (1.39 \pm 0.09 \pm 0.05)$  ps has been measured. The main systematic errors arise from the background shape and from non- $B_S^0$  backgrounds. In the Standard Model of the CKM mixing matrix, the ratio  $\Delta\Gamma/\Delta m$  contains no CKM matrix elements and depends only on QCD corrections. If the error on this QCD calculation is understood and not too large, a measurement of  $\Delta\Gamma$  in the  $B_S^0$  meson system implies a determination of  $\Delta m_S$  and thus a way to infer  $B_S^0\bar{B}_S^0$  mixing. The  $B_S^0$  meson proper decay length distribution has been examined for a lifetime difference  $\Delta\Gamma/\Gamma$  between the two  $CP$  eigenstates of the  $B_S^0$  meson,  $B_S^H$  and  $B_S^L$ . Instead of fitting for a functional form of  $\Gamma e^{-\Gamma t}$  the likelihood fit has been expanded to fit for a functional form  $1/2 \cdot (\Gamma_L e^{-\Gamma_L t} + \Gamma_H e^{-\Gamma_H t})$  with  $\Gamma_{L,H} = \Gamma \pm \Delta\Gamma/2$ . Fixing the average  $B_S^0$  lifetime to the PDG value  $\tau(B_S^0) = (1.57 \pm 0.08)$  ps [18], the fit returns  $\Delta\Gamma/\Gamma = 0.48^{+0.26}_{-0.48}$  indicating that the current statistics is not sensitive to a  $B_S^0$  lifetime difference. Based on this fit result a limit on  $\Delta\Gamma/\Gamma < 0.81$  (95% CL) can be set. Using a value of  $\Delta\Gamma/\Delta m = (5.6 \pm 2.6) \cdot 10^{-3}$  from [21], an upper limit on the  $B_S^0$  mixing frequency  $\Delta m_S$  can be obtained

$$\Delta m_S < 92 \times (5.6 \cdot 10^{-3}) / (\Delta\Gamma/\Delta m) \times (1.57 \text{ ps} / \tau_{B_S^0}) \quad (95\% \text{ CL}).$$

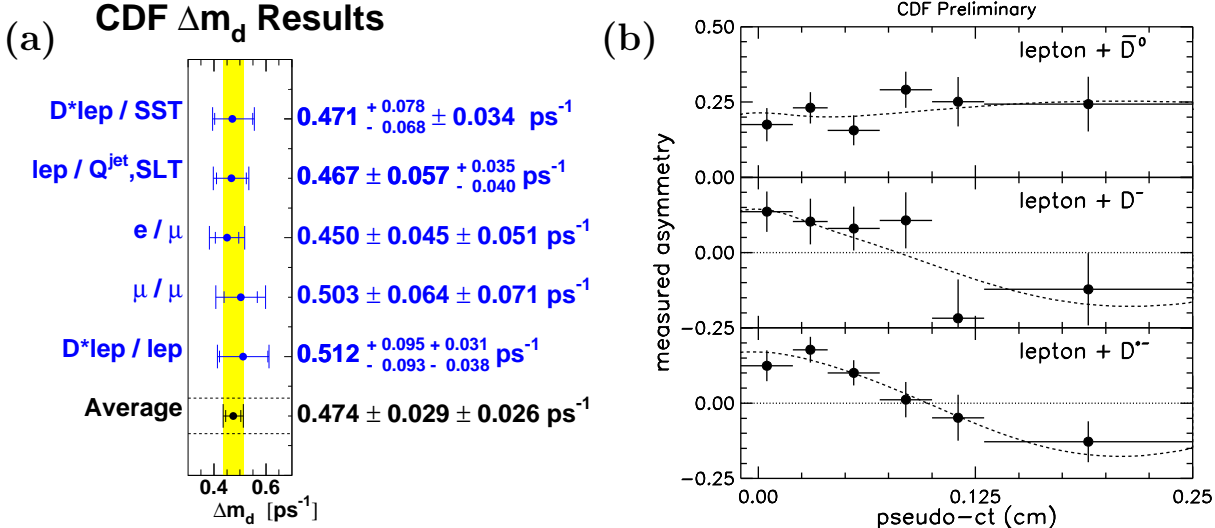


Figure 6: (a) Summary of time dependent  $\Delta m_d$  results from CDF. (b) Measured asymmetry from the  $D^{(*)}\ell$  mixing analysis.

### 3.2 $B^0 \bar{B}^0$ Oscillations

In the Standard Model,  $B^0 \bar{B}^0$  mixing occurs through a second order weak process, where the dominant contribution is through a top quark loop. The oscillation is expressed in terms of its frequency  $\Delta m_d$ , where  $\Delta m_d$  is the difference in mass between the two  $B^0$  meson eigenstates. For a beam initially pure in  $B^0$  mesons at  $t = 0$ , the number of  $B^0$  that oscillate at proper time  $t$  is given by  $N(t)_{B^0 \rightarrow \bar{B}^0} = 1/2 \Gamma \exp(-\Gamma t) \cdot (1 - \cos \Delta m_d t)$ . Measurements of the frequencies of  $B^0$  and  $B_S^0$  oscillations can constrain the magnitudes of the CKM matrix elements  $V_{td}$  and  $V_{ts}$ .

In general, a time dependent mixing measurement requires the knowledge of the flavour of the  $B$  meson at production and at decay, as well as the proper decay time of the  $B$  meson. Experimentally, the flavour of the  $B$  meson at decay time is determined from the observed decay products like the charge of the lepton from a semileptonic  $B$  decay. The flavour at production time can be determined in various ways, employing either the second  $b$ -flavoured hadron in the event, or the charge correlation with particles produced in association with the  $B^0$  meson ('same side tagging' SST). CDF has preliminary results on several time-dependent  $B^0$  mixing analyses utilizing several ways to tag the  $B$  flavour at production. These measurements include opposite side lepton tagging, jet charge tagging, or SST as can be seen in Fig. 6a). The combined average from the CDF  $\Delta m_d$  measurements is  $\Delta m_d = (0.474 \pm 0.029 \pm 0.026) \text{ ps}^{-1}$ , which is competitive with results from other experiments [18]. In the following, we report about one of CDF's  $\Delta m_d$  measurements exploiting the same side tag, which is of particular interest at a hadron collider.

#### 3.2.1 $B^0 \bar{B}^0$ Mixing in $D^{(*)}\ell$ Events

For this analysis, further described in Ref. [22],  $B$  mesons are reconstructed through their semileptonic decays  $B \rightarrow D^{(*)}\ell\nu X$ . The analysis starts with single lepton trigger data and reconstructs  $D^{(*)}$  meson candidates in a cone around the trigger electron or muon in the following channels:  $\bar{B}^0 \rightarrow D^{*+}\ell^-\nu$ ,  $D^{*+} \rightarrow D^0\pi^+$  with  $D^0 \rightarrow K^-\pi^+$ ,  $K^-\pi^+\pi^+\pi^-$ , and  $K^-\pi^+\pi^0$  ( $\pi^0$  not reconstructed) as well as  $\bar{B}^0 \rightarrow D^+\ell^-\nu$ ,  $D^+ \rightarrow K^-\pi^+\pi^+$ , and  $B^- \rightarrow D^0\ell^-\nu$ , with  $D^0 \rightarrow K^-\pi^+$  (veto  $D^{*+}$ ). About 7000 partially reconstructed  $B^0$  mesons

and about 2000  $B^+$  candidates are selected this way. The  $D^{(*)}$  candidates are intersected with the lepton to find the  $B$  decay vertex in a similar way as described in Sec. 3.1.1. To tag the  $B$  flavour at production, a same side tagging algorithm, which exploits the correlation between the  $B$  flavour and the charge of tracks from either the fragmentation process or  $B^{**}$  resonances [23], is used. In this analysis no attempt is made to differentiate the sources of correlated pions. To study the correlation between the flavour of the  $B$  meson and the charged particles produced in association with it, all tracks within a  $\eta$ - $\phi$  cone of radius 0.7 centered around the direction of the  $D^{(*)}\ell$  candidate are used. The tracks considered as tags should be consistent with the hypothesis that they originate from the fragmentation chain or the decay of  $B^{**}$  mesons; this means they are required to come from the primary event vertex.

String fragmentation models indicate that the velocity of the fragmentation particles is close to the velocity of the  $B$  meson. Similarly, pions from  $B^{**}$  decays should also have a velocity close to the one of the  $B$  meson. In particular, the relative transverse momentum ( $p_t^{\text{rel}}$ ) of the particle with respect to the combined momentum of the  $D^{(*)}\ell$  combination plus tag particle momentum, should be small. Of the candidate tracks, we select as the tag the track that has the minimum component of momentum  $p_t^{\text{rel}}$  to the momentum sum of that track, and the  $D^{(*)}\ell$  combination. The efficiency for finding such a tag is  $\sim 70\%$ . Since we know the flavour of the  $B$  meson at decay from the  $D^{(*)}\ell$  signature, we compare the number of right-sign ( $N_{RS}$ ) SST tags to the number of wrong-sign ( $N_{WS}$ ) tags as a function of  $c\tau$ . For the  $B^0$  meson we expect the asymmetry  $A(t)$  to be  $A(t) = (N_{RS}(t) - N_{WS}(t))/(N_{RS}(t) + N_{WS}(t)) = D \cdot \cos(\Delta m_d t)$ , where  $D$  is the dilution of the same side tagging algorithm.  $D$  is also related to the probability  $w$  of mistagging the flavour by  $D = 1 - 2w$ . In this analysis both  $\Delta m_d$  and  $D$  are determined simultaneously.

To obtain the asymmetry for  $B^0$  and  $B^+$  mesons, a correction is applied for the fact that each  $D^{(*)}\ell$  signal has contributions from both neutral and charged  $B$  mesons via  $D^{**}$  decays. The fit result is shown in Fig. 6b). The fit yields  $\Delta m_d = (0.471^{+0.078}_{-0.068} \pm 0.034) \text{ ps}^{-1}$ , as well as the neutral and charged dilutions  $D_0 = 0.18 \pm 0.03 \pm 0.02$  and  $D_+ = 0.27 \pm 0.03 \pm 0.02$ , respectively.

## 4 Conclusions

In this article, we have reviewed recent heavy quark physics results from the Tevatron  $p\bar{p}$  collider at Fermilab. We summarized the status of top quark physics at CDF and DØ including measurements of the top production cross section and the top quark mass in several top decay modes. We also discussed recent  $B$  physics results from the CDF experiment including  $B$  hadron lifetime measurements, which are very competitive with the LEP and SLC results, as well as time dependent  $B^0\bar{B}^0$  mixing. These results give rise to good prospects of top and  $B$  physics at the Tevatron in Run II starting in 1999.

## Acknowledgments

It is a pleasure to thank all friends and colleagues from the CDF and DØ collaboration for their excellent work and their help in preparing this talk. Special thanks go to M. Beyer, T. Mannel and H. Schröder for organizing such a delightful workshop. A constant source of inspiration and support is my wife Ann, who I like to thank for her love and her continuous understanding about the life of a physicist.

## References

- [1] F. Abe et al. (CDF), Nucl.Instr.Methods **A271** (1988) 387, and references therein.
- [2] S. Abachi et al. (D $\emptyset$ ), Nucl.Instr.Methods **A338** (1994) 185, and references therein.
- [3] E. Laenen, J. Smith, and W.L. Van Neerven, Nucl.Phys. **B369** (1992) 543, Phys.Lett. **B321** (1994) 254.
- [4] B. Abbott et al. (D $\emptyset$ ), Fermilab-Pub-97/172-E (1997).
- [5] F. Abe et al. (CDF), Fermilab-Pub-97/304-E (1997).
- [6] S. Abachi et al. (D $\emptyset$ ), Phys.Rev.Lett. **79** (1997) 1203.
- [7] F. Abe et al. (CDF), Phys.Rev.Lett. **79** (1997) 3585.
- [8] F. Abe et al. (CDF), Phys.Rev. **D50** (1994) 2966.
- [9] F. Abe et al. (CDF), Phys.Rev.Lett. **74** (1995) 2626.
- [10] S. Abachi et al. (D $\emptyset$ ), Phys.Rev.Lett. **74** (1995) 2632.
- [11] S. Abachi et al. (D $\emptyset$ ), Phys.Rev.Lett. **79** (1997) 1197.
- [12] F. Abe et al. (CDF), Phys.Rev.Lett. **79** (1997) 1992.
- [13] F. Abe et al. (CDF), Fermilab-Pub-97/286-E (1997).
- [14] P. Nason, S. Dawson, and R.K. Ellis, Nucl.Phys. **B303** (1988) 607; E.L. Berger and H. Contopanagos, Phys.Rev. **D54** (1996) 3085; S. Catani et al., Phys.Lett. **B378** (1996) 329.
- [15] F. Abe et al. (CDF), Fermilab-Pub-97/284-E (1997).
- [16] N. Cabibbo, Phys.Rev.Lett. **10** (1963) 531; M. Kobayashi, T. Maskawa, Prog.Theor.Phys. **49** (1973) 652.
- [17] C. Albajar et al. (UA 1), Phys.Lett. **B186** (1987) 247; Phys.Lett. **B256** (1991) 221; erratum: *ibid*, **B262** (1991) 497.
- [18] R.M. Barnett et al. (Particle Data Group), Phys.Rev. **D54** (1996) 1, and 1997 off-year partial update available on the PDG WWW pages (URL: <http://pdg.lbl.gov/>).
- [19] M.B. Voloshin and M.A. Shifman, Sov.Phys.JETP **64**, 698 (1986); I.I. Bigi and N.G. Uraltsev, Phys.Lett. **B280** (1992) 271; I.I. Bigi, Nuovo Cim. **A109** (1996) 713.
- [20] M. Neubert, Int.J.Mod.Phys. **A11** (1996) 4173; M. Neubert, C.T. Sachrajda, Nucl.Phys. **B483** (1997) 339.
- [21] M. Beneke, G. Buchalla, and I. Dunietz, Phys.Rev. **D54** (1996) 4419.
- [22] F. Abe et al. (CDF), Fermilab-Pub-97/312-E (1997).
- [23] M. Gronau, A. Nippe and J. Rosner, Phys.Rev. **D47** (1993) 1988.